Supporting Information

Crystal size versus paddle wheel deformability: selective gated adsorption transitions of the switchable metal-organic frameworks DUT-8(Co) and DUT-8(Ni)

Sebastian Ehrling[a], Irena Senkovska*[a], Volodymyr Bon[a], Jack D. Evans[a], Petko Petkov[b], Yulia Krupskaya[c], Vladislav Kataev[c], Toshiki Wulf[d,e], Alexander Krylov[f], Alexander Vtyurin[f,g], Svetlana Krylova[f], Sergey Adichtchev[h], Evgenia Slyusareva[g], Manfred S. Weiss[i], Bernd Büchner[c], Thomas Heine[e,j] and Stefan Kaskel*[a]

Content

1. Rietveld plot of the closed phase of DUT-8(Co), 1a_cp

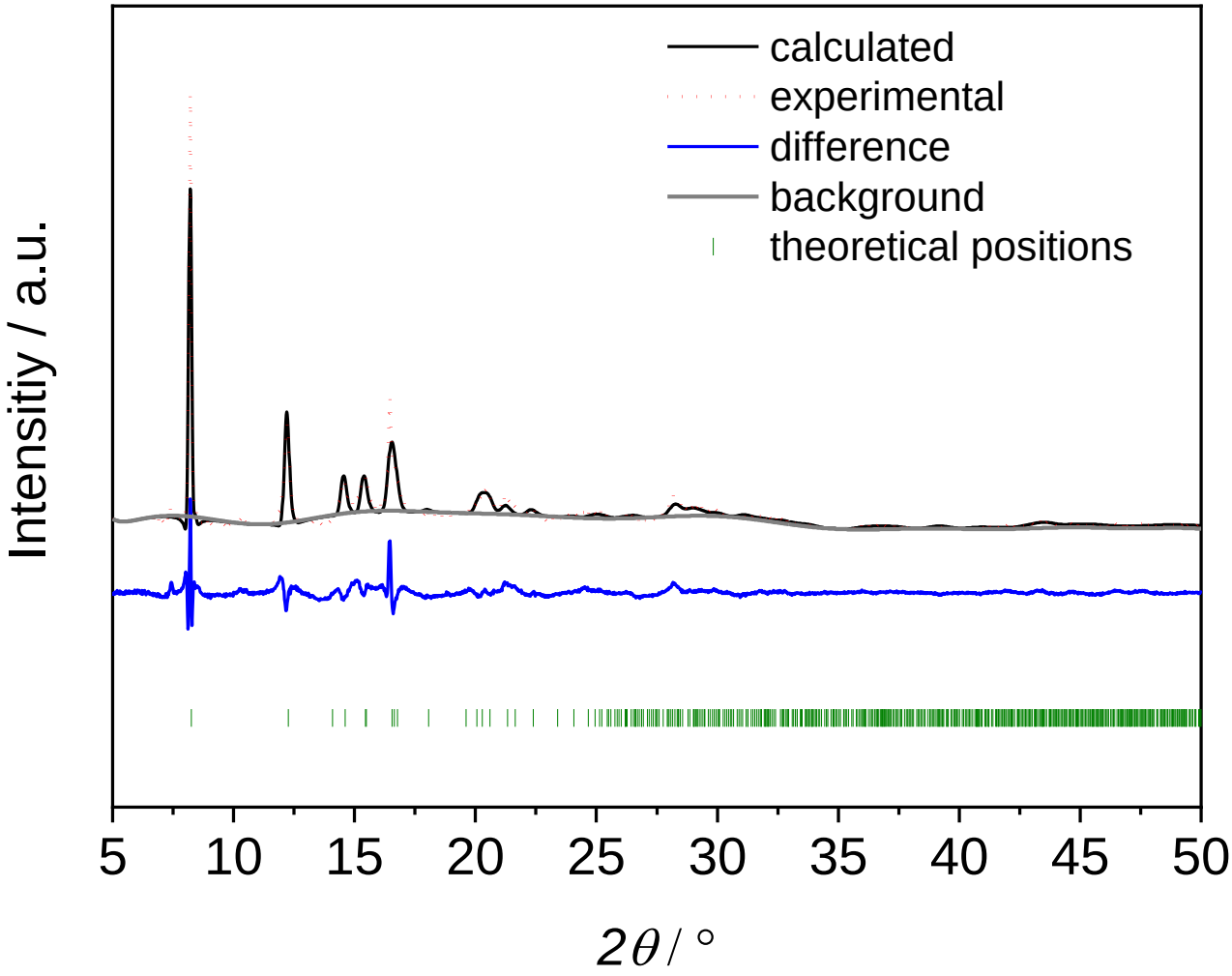

Figure S1. Rietveld refinement plot of closed pore phase of DUT-8(Co) (**1a**_*cp*).

2. Additional SEM images

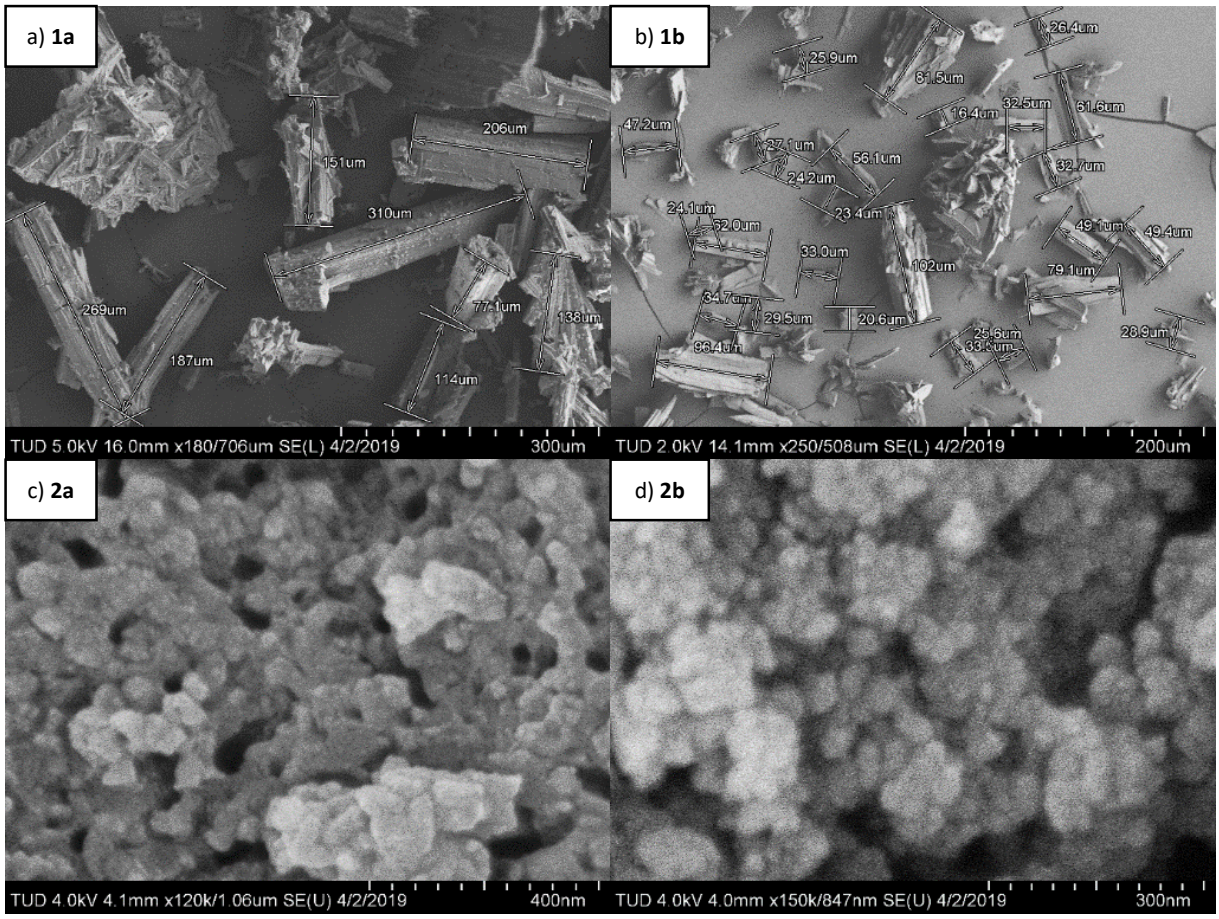

Figure S2. SEM images of a) **1a**_*cp*, b) **1b**_*cp*, c) **2a**_*op*, d) **2b**_*op.* Magnification is displayed directly in the picture.

The particle size distribution of all samples was investigated by SEM. It revealed that the biggest particles of **1a** (300 µm) are three times bigger compared to **1b** (100 µm). Both samples show presence of particles in a second size regime, between 20 – 50 µm. The submicron-sized particles of **2a** are around 100 nm, whilst the particles of **2b** have a maximum size of ca. 70 nm.

3. Thermogravimetric analysis

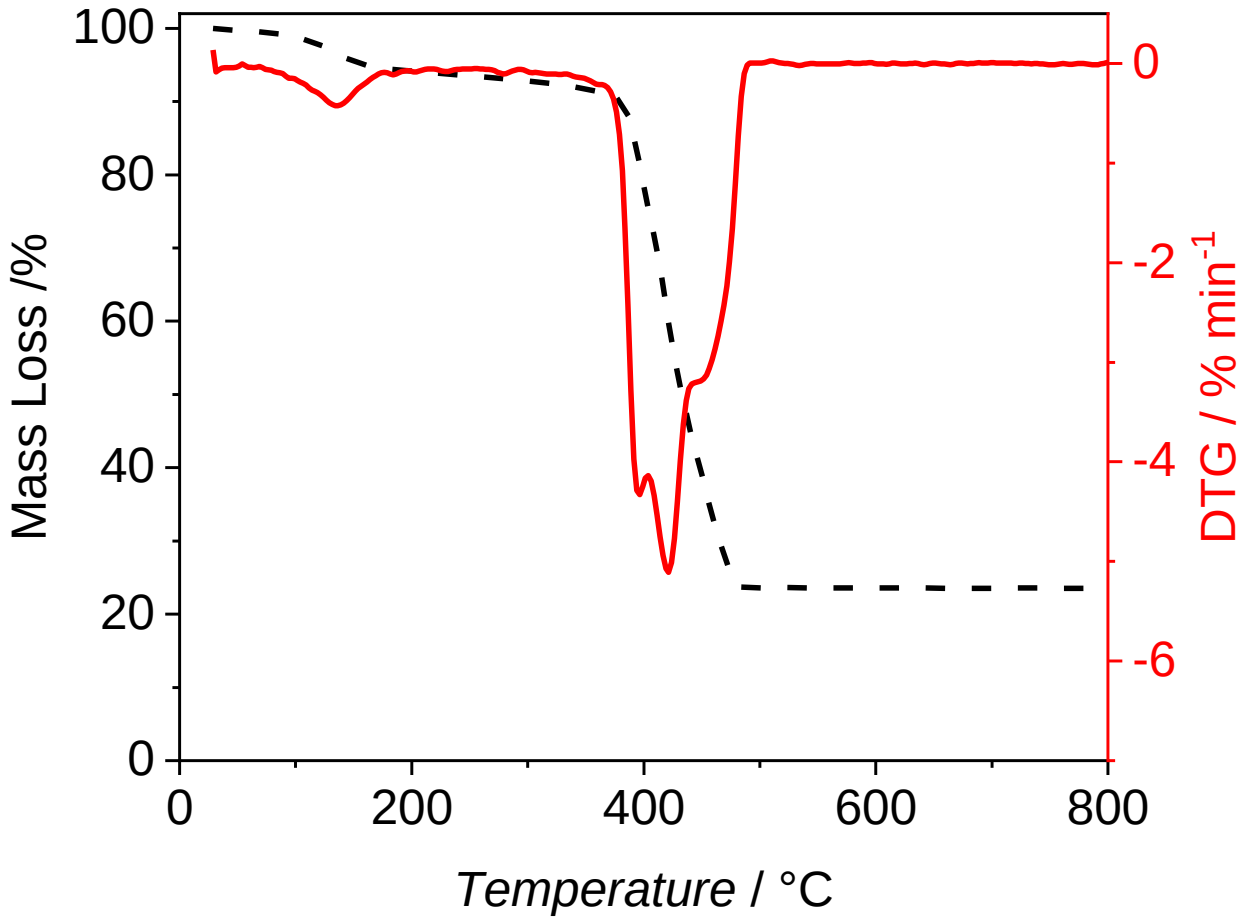

Figure S3. TGA of **1a** (macro-sized DUT-8(Co)) in air with a heating rate of 5 K min^{-1}.

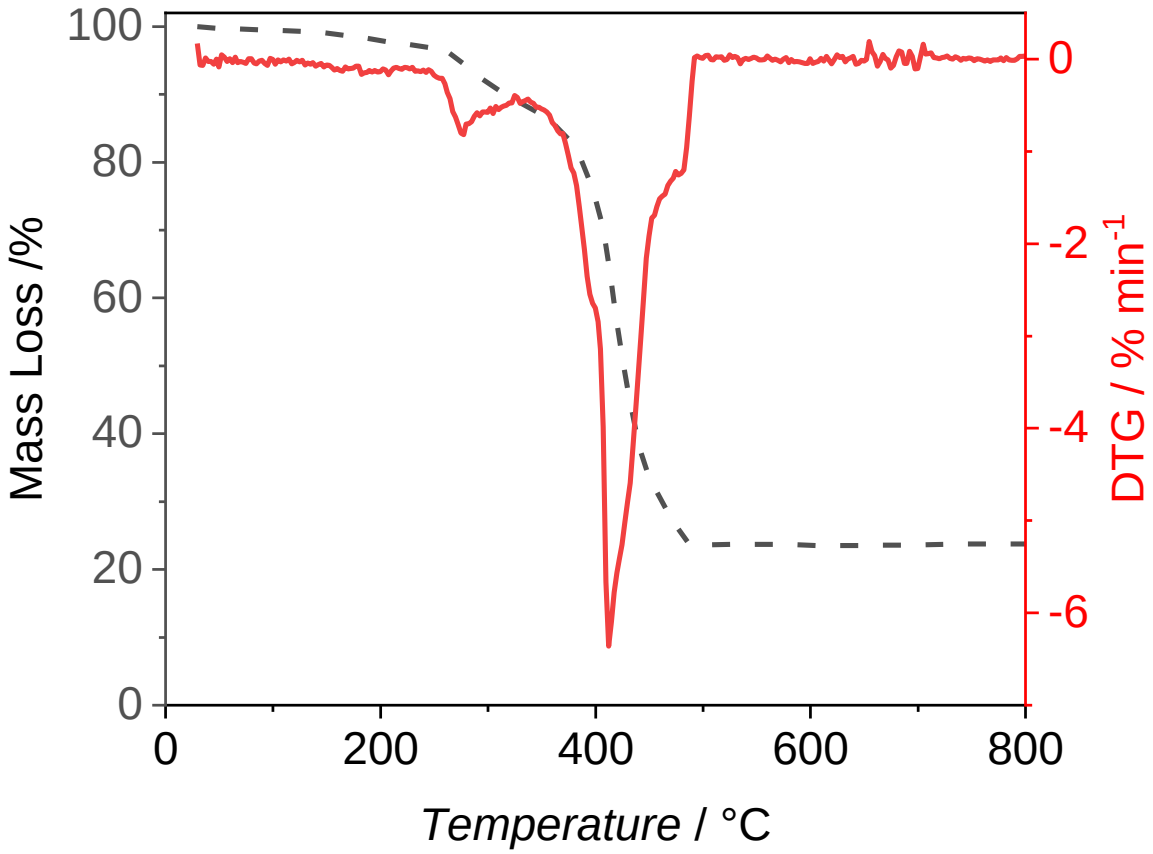

Figure S4. TGA of **2a** (submicron-sized DUT-8(Co)) in air with a heating rate of 5 K min^{-1}.

4. Additional gas adsorption experiments

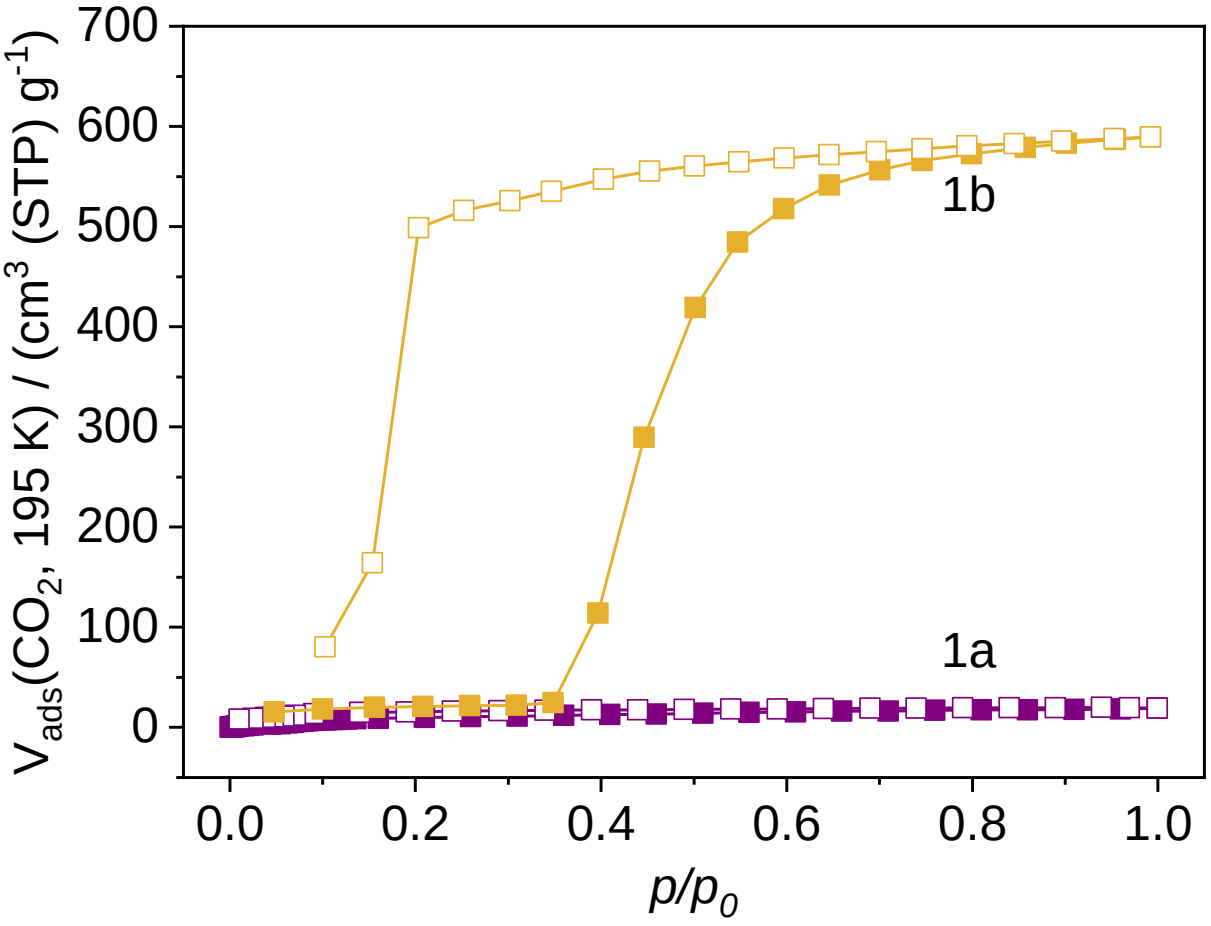

Figure S5. CO_2 physisorption at 195 K on **1a** and **1b**. Filled symbols – adsorption, open symbols – desorption.

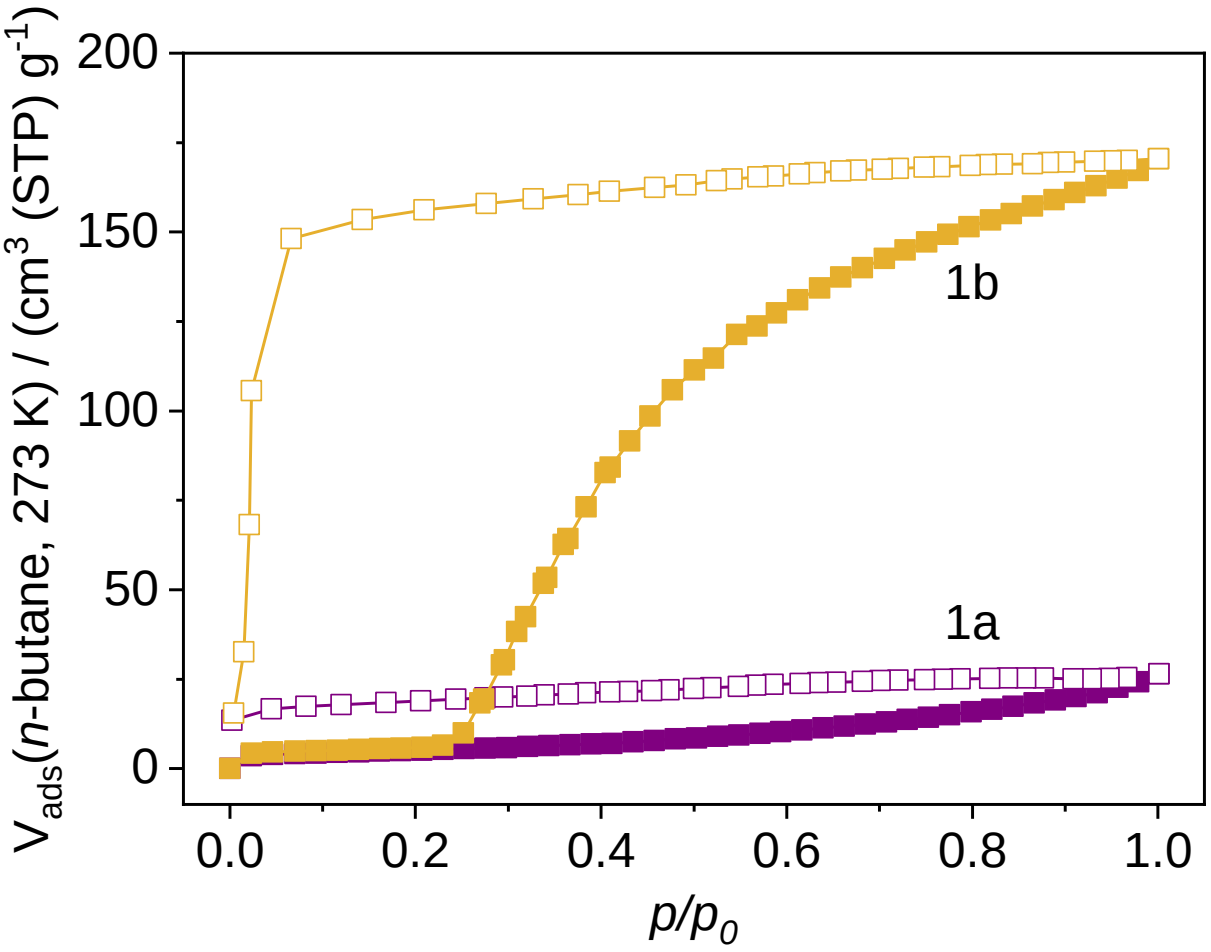

Figure S6. *n*-Butane physisorption at 273 K on **1a** and **1b**. Filled symbols – adsorption, open symbols – desorption.

5. Additional PXRD experiments

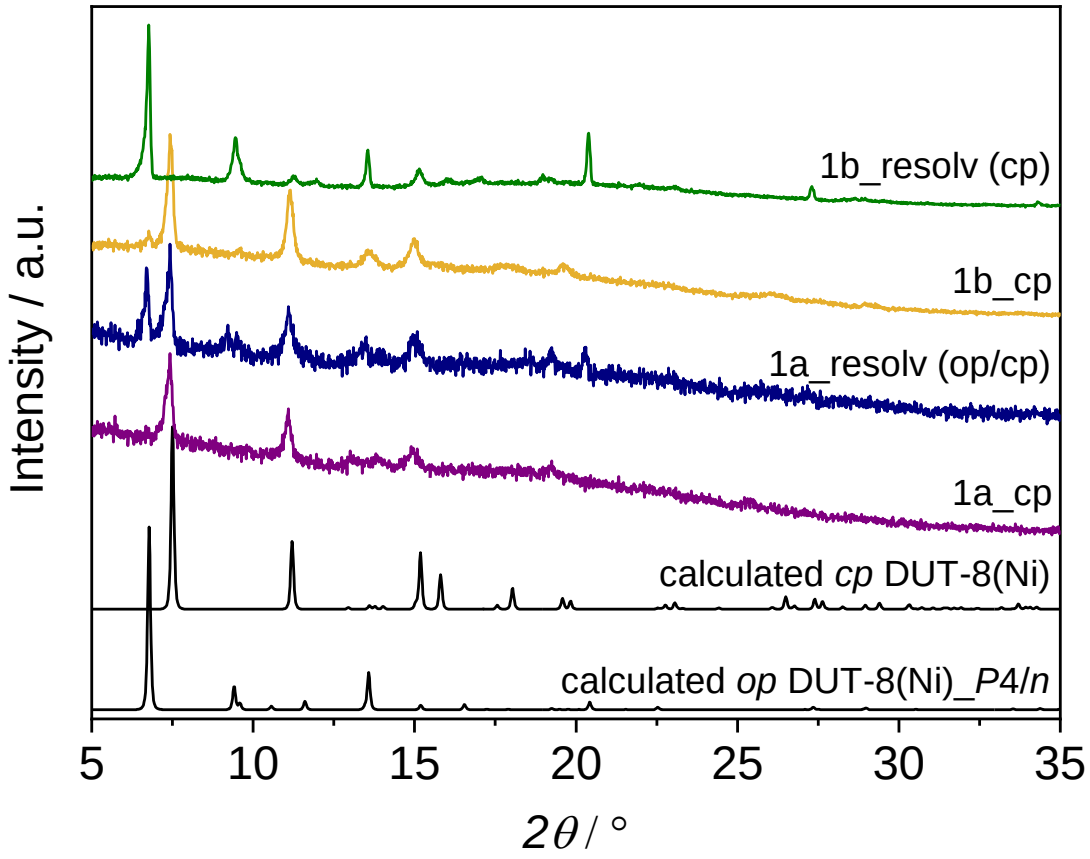

Figure S7. PXRD patterns of desolvated macro-sized samples **1a**_*cp* and **1b**_*cp* and after resolvation in DMF.

6. Additional vapour adsorption experiments

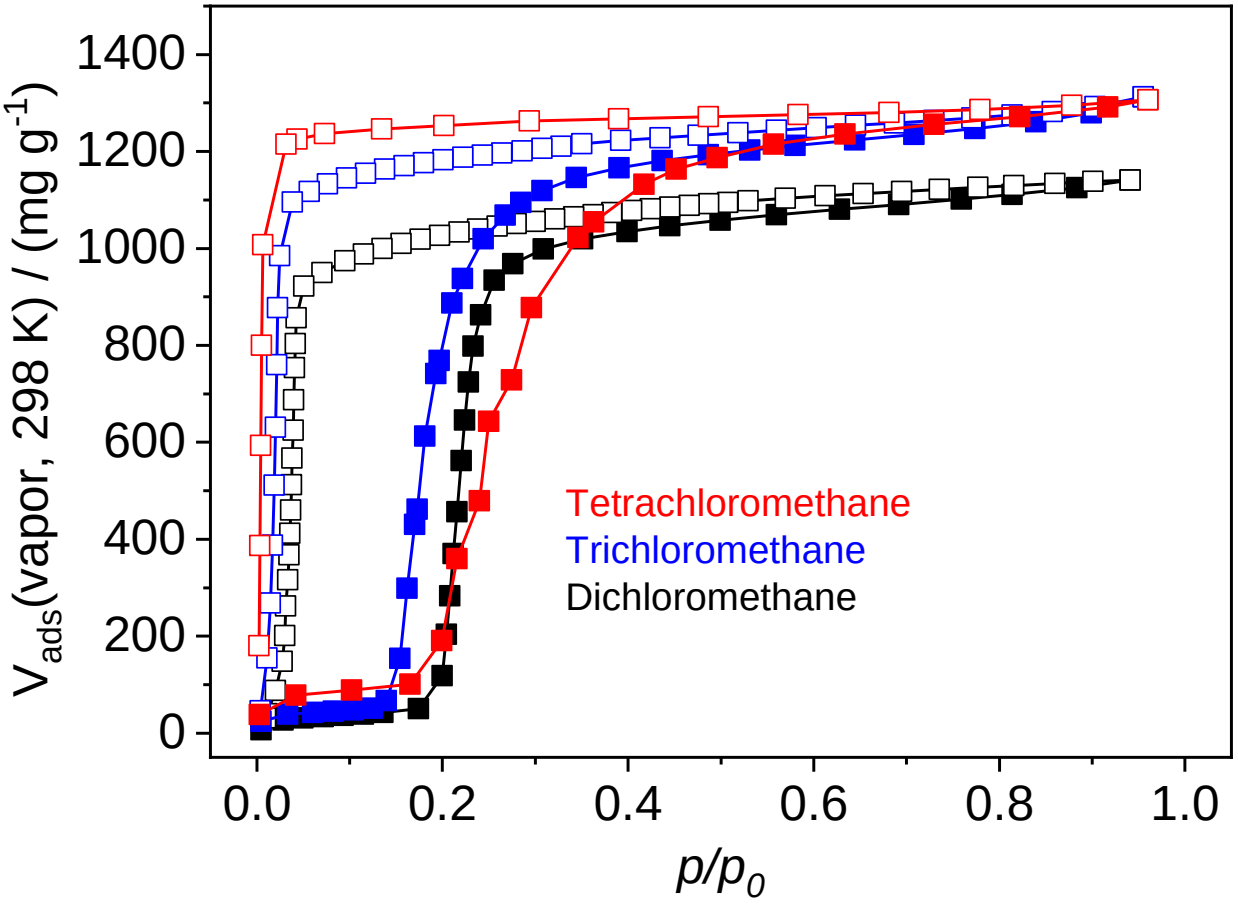

Figure S8. Physisorption isotherms of chlorinated methanes on **1b**_*cp* at 298 K. Filled symbols – adsorption, open symbols – desorption.

7. Heat of adsorption determination

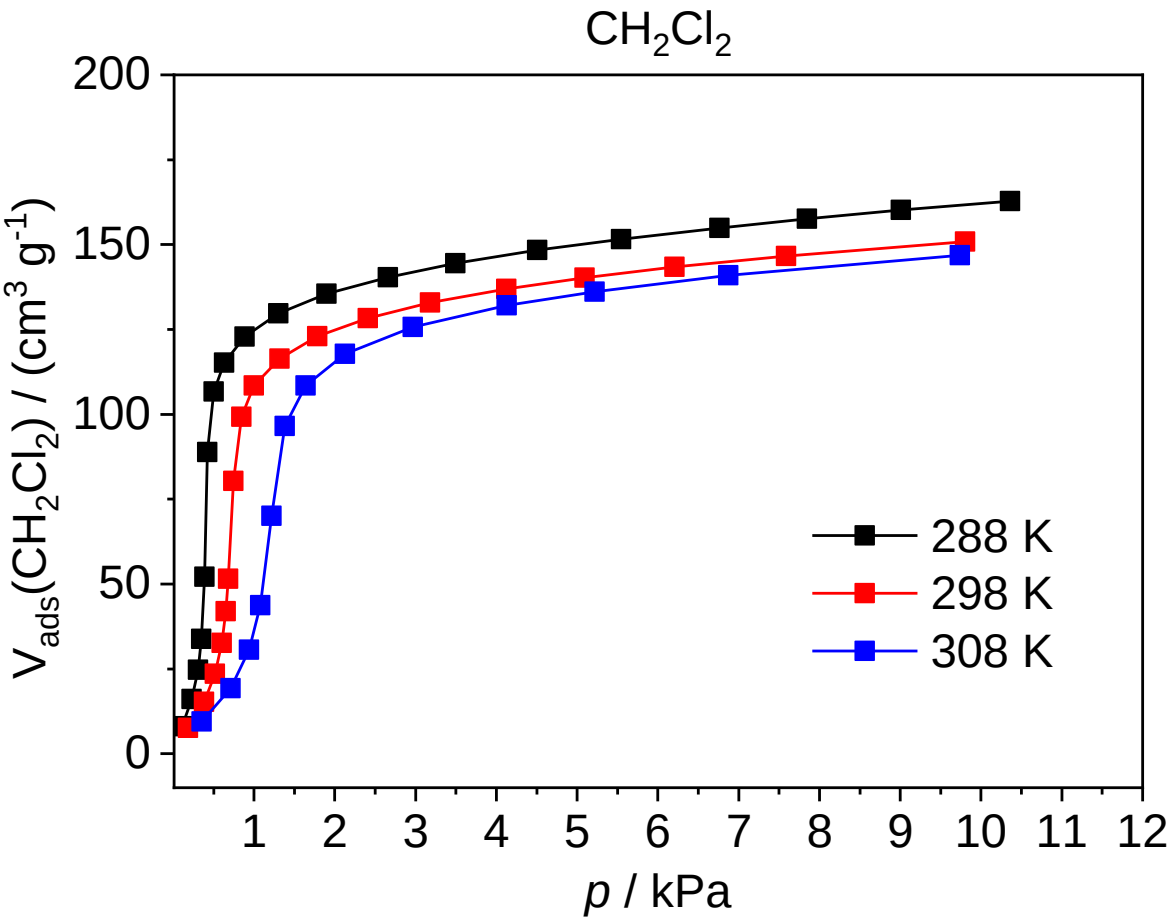

Figure S9. Vapor adsorption of CH_2Cl_2 at 288 K, 298 K and 308 K on **2b**.

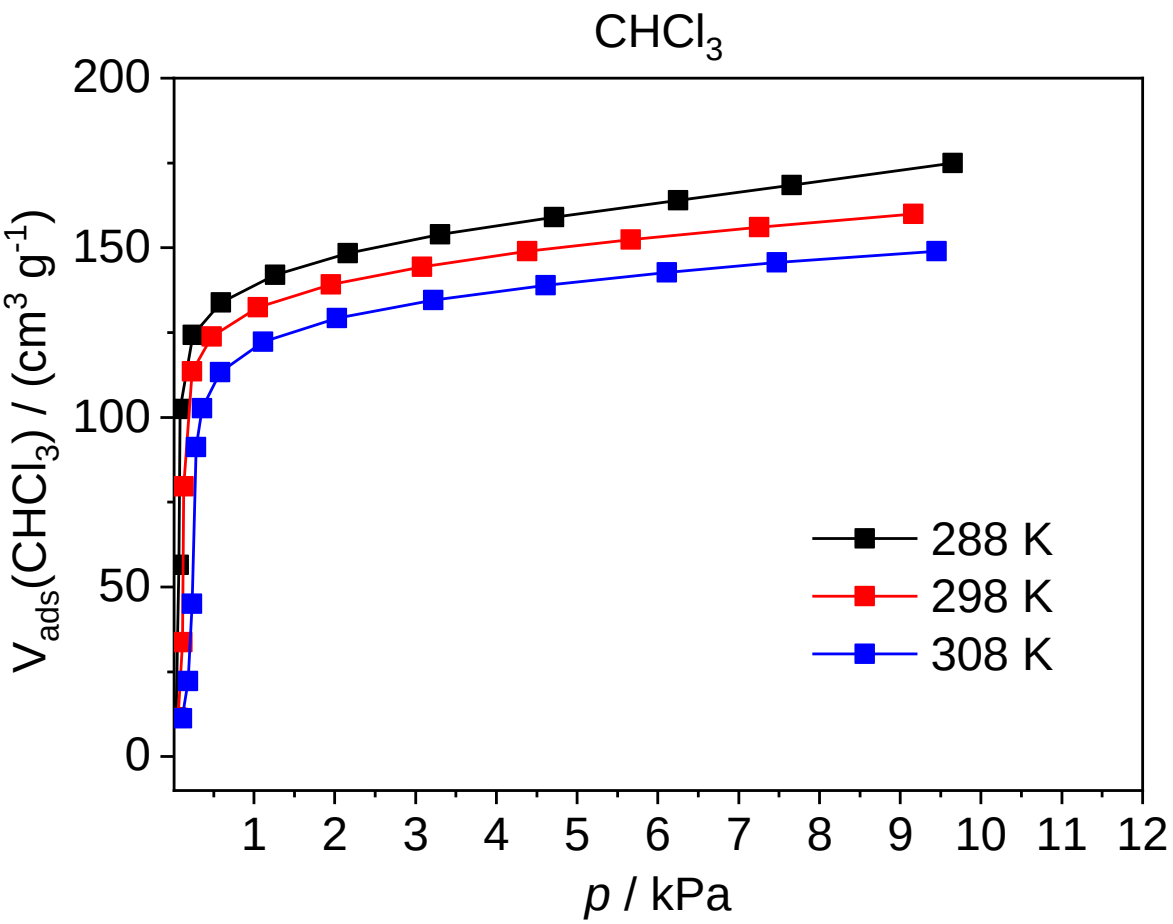

Figure S10. Vapor adsorption of $CHCl_3$ at 288 K, 298 K and 308 K on **2b**.

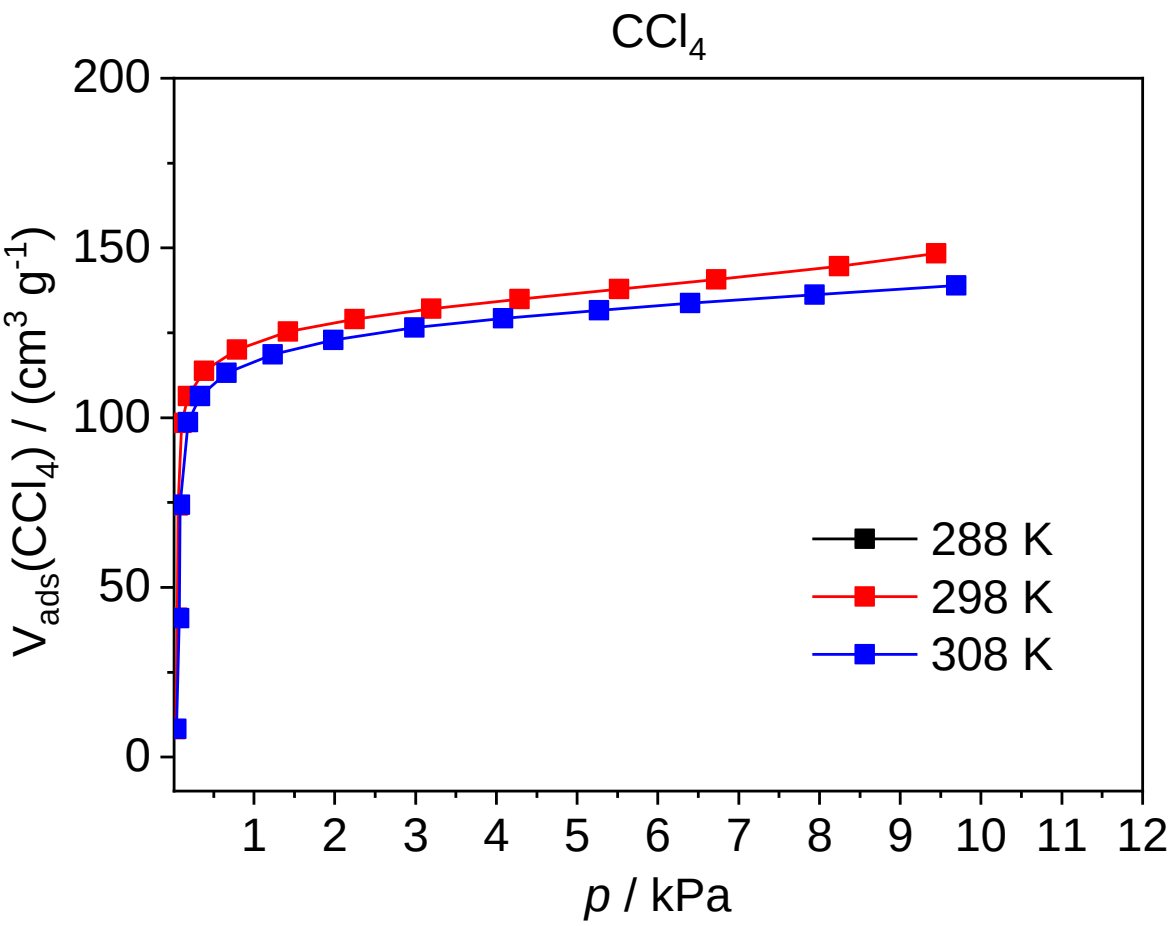

Figure S11. Vapor adsorption of CCl_4 at 288 K, 298 K and 308 K on **2b**.

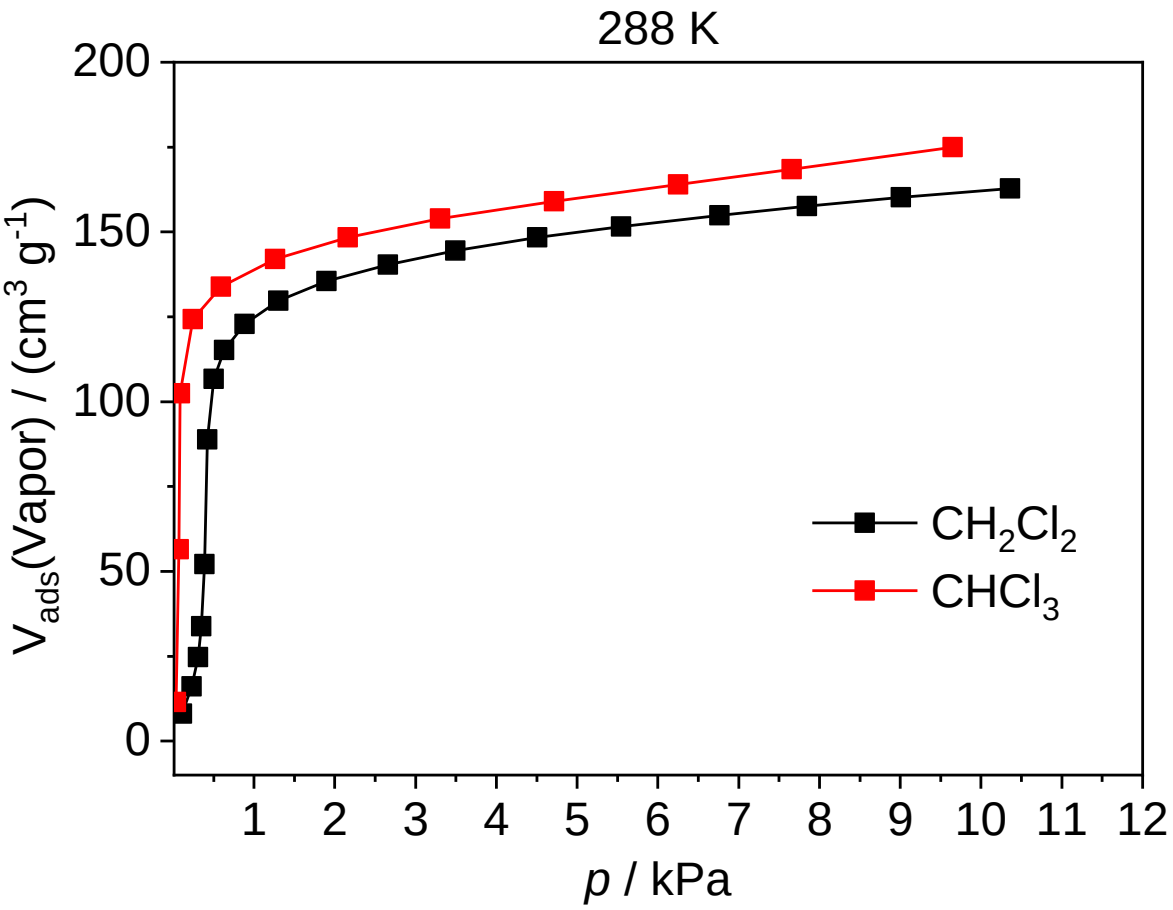

Figure S12. Adsorption of CH_2Cl_2 and $CHCl_3$ at 288 K on **2b**.

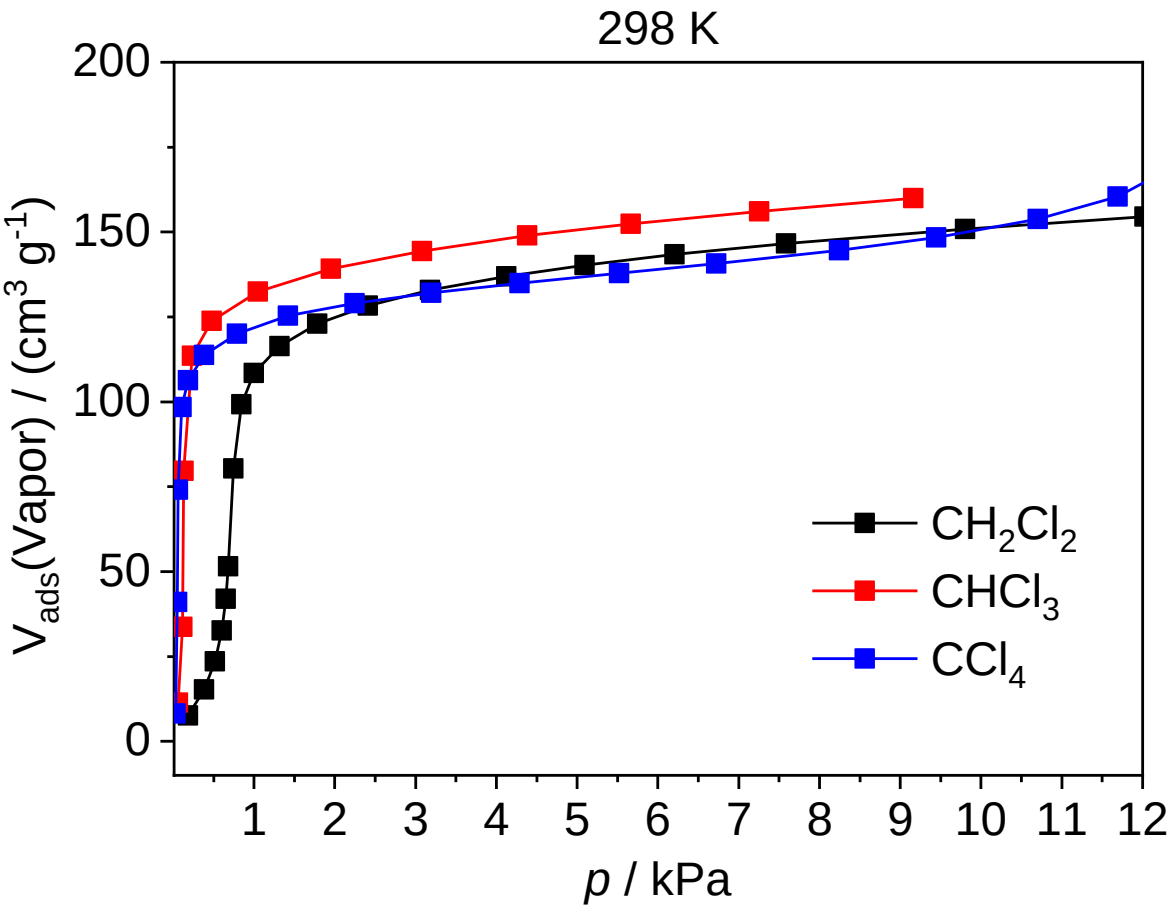

Figure S13. Adsorption of CH_2Cl_2 and $CHCl_3$ and CCl_4 at 298 K on **2b**.

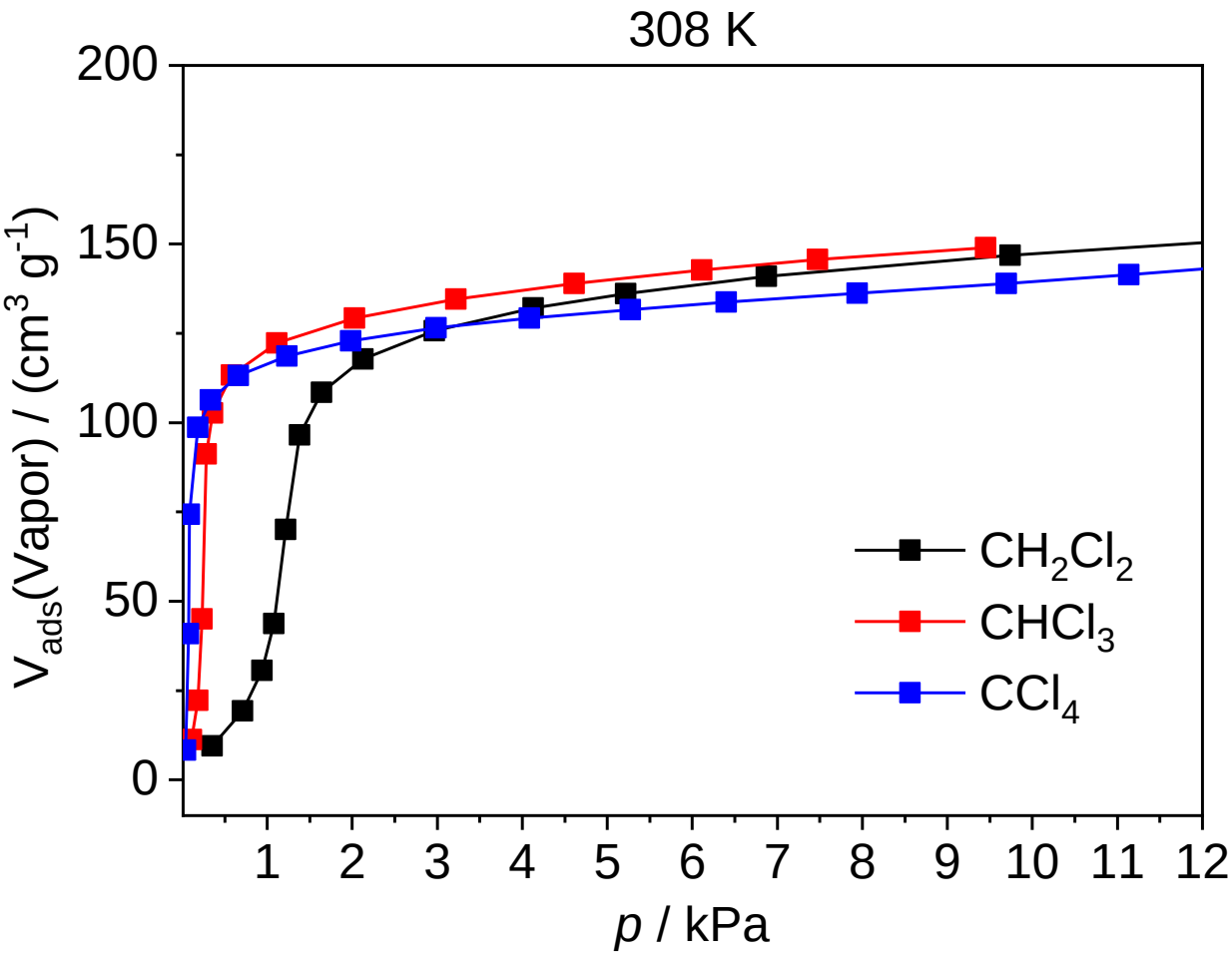

Figure S14. Adsorption of CH_2Cl_2 and $CHCl_3$ and CCl_4 at 308 K on **2b**.

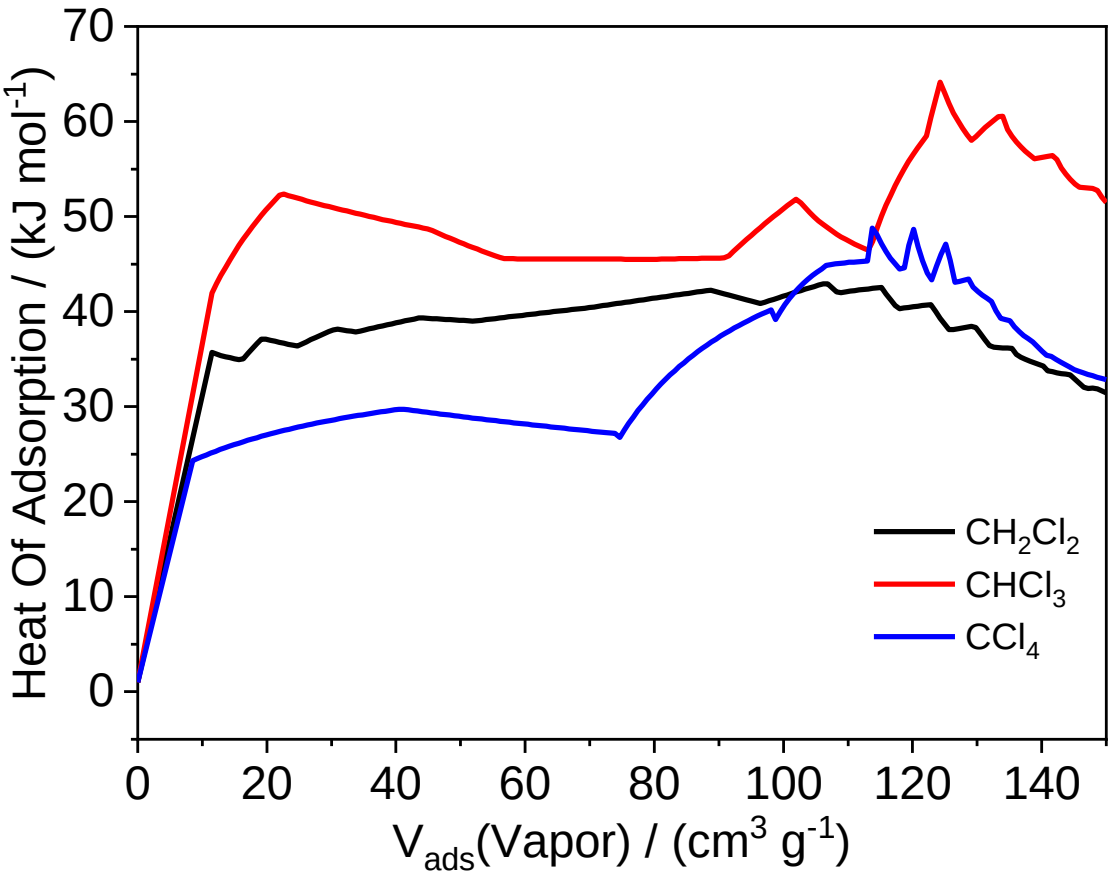

Figure S15. Isosteric heat of adsorption for CH_2Cl_2, $CHCl_3$ and CCl_4 as a function of the loading.

8. Additional crystallographic figures

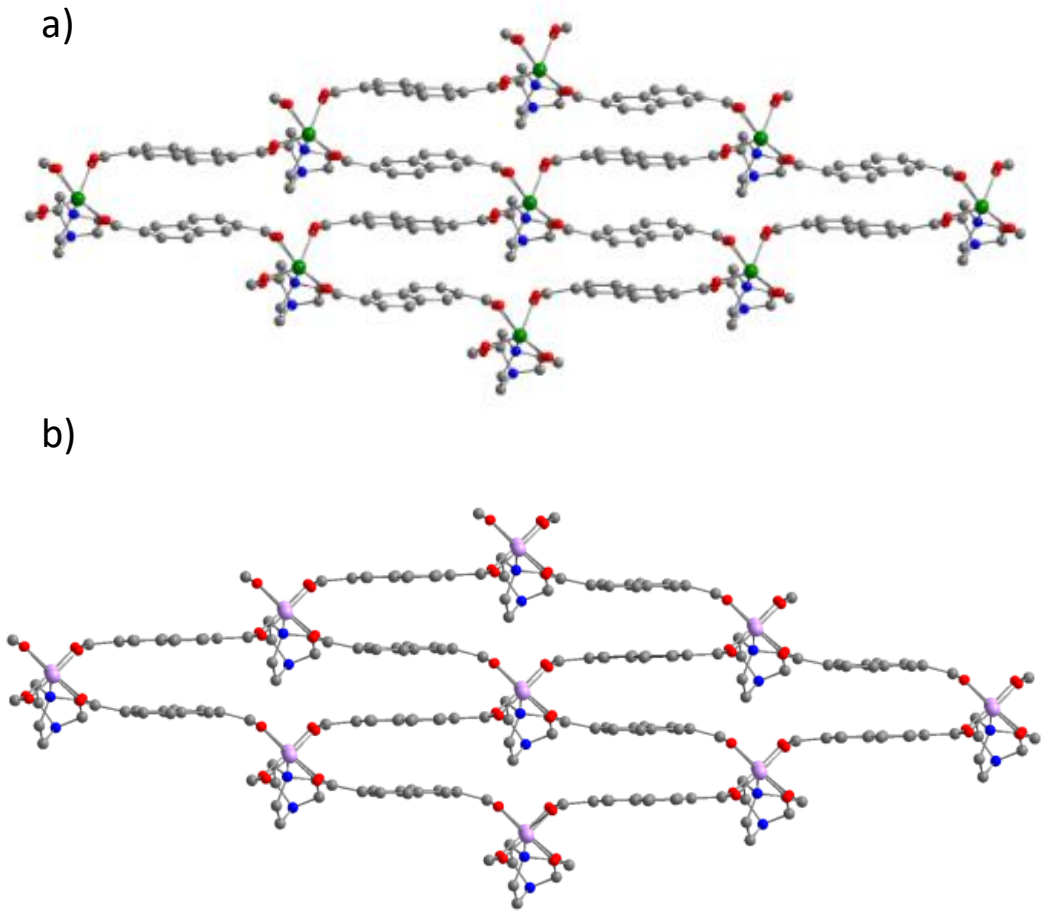

Figure S16. Crystal structure of a) **1b**_*cp* and b) **1a**_*cp*. View along the channels.
C – in grey, O – in red, N – in blue, Ni – in green, Co – in purple. Hydrogen atoms are omitted.

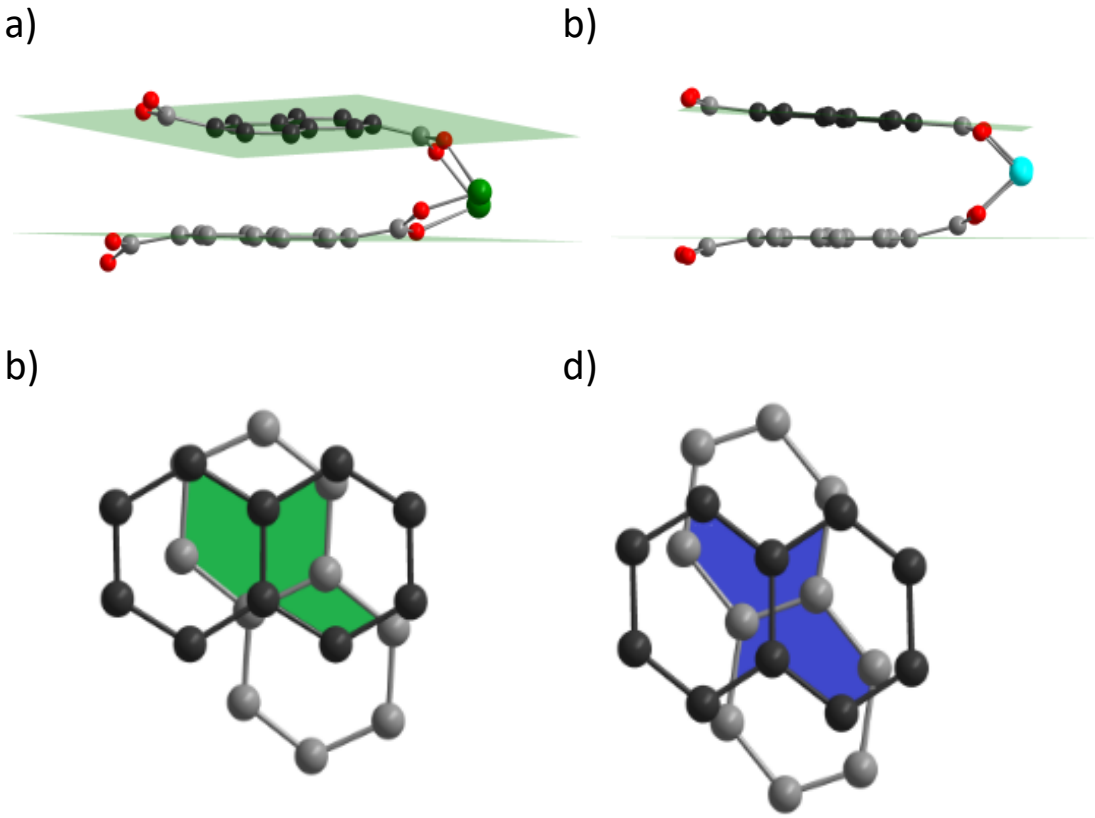

Figure S17. The alignment of the linkers in a) **1b**_*cp* and b) **1a**_*cp*. Furthermore, the alignment of the naphthalene cores in c) **1b**_cp and d) **1a**_*cp* are shown. The coloured areas represent the overlap of the two p-rings. C – in grey/black, O – in red, N – in blue, Ni – in green, Co – in violet. Hydrogen atoms are omitted.

9. Infrared Spectroscopy

The additional band at 1672 cm^{-1} in 2a_*desolv* can be assigned to residual DMF in the pore channels.

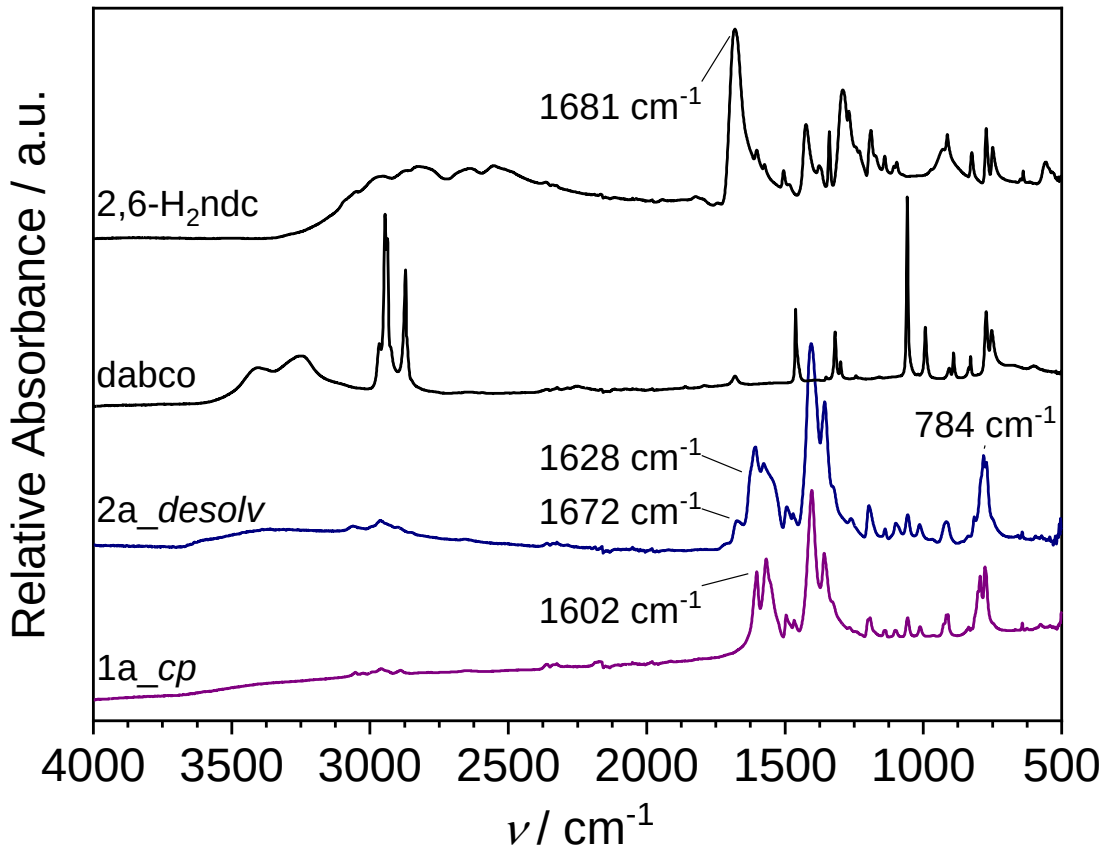

Figure S18. FT-IR spectra of macro-sized particles of DUT-8(Co) (violet, **1a**_*cp*), submicron-sized particles of DUT-8(Co) (blue, **2a**_*desolv*), dabco and 2,6-H_2ndc.

10. Raman Spectroscopy

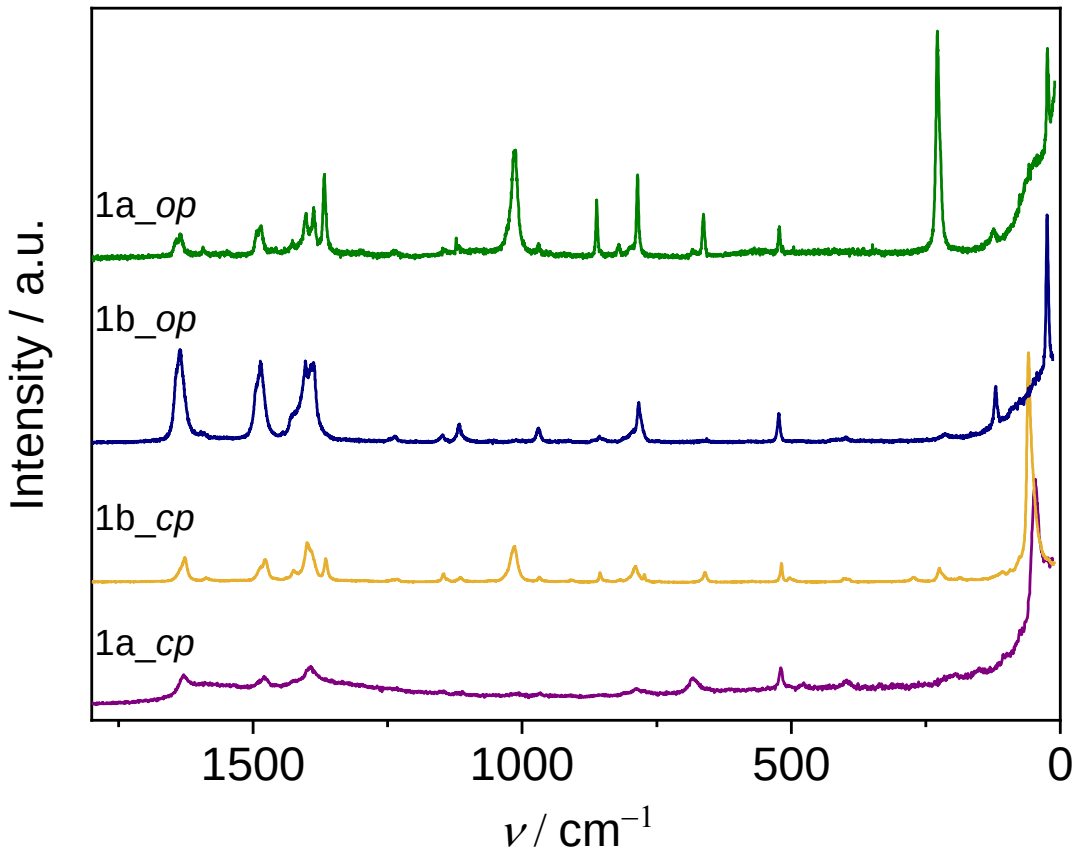

Figure S 19. Raman spectra of 1a_*op* (blue), 1b_*op* (green), 1a_*cp* (purple) and 1b_*cp* (yellow).

11. Spin related cluster optimization

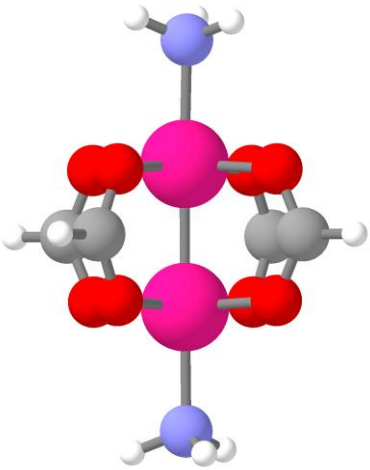

Figure S20. Structure of the Co paddle wheel cluster molecular analogue.

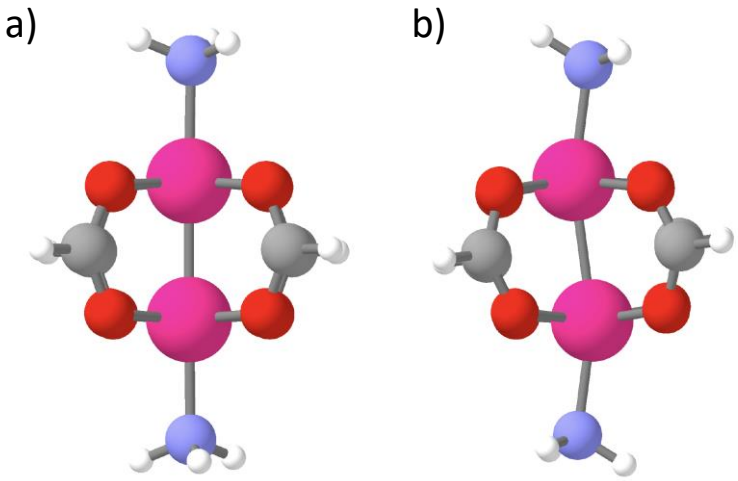

Figure S21. Optimised structures of the Co paddle wheel in the a) low-spin state, 2S+1 = 1, and b) 2S+1 = 3 state.

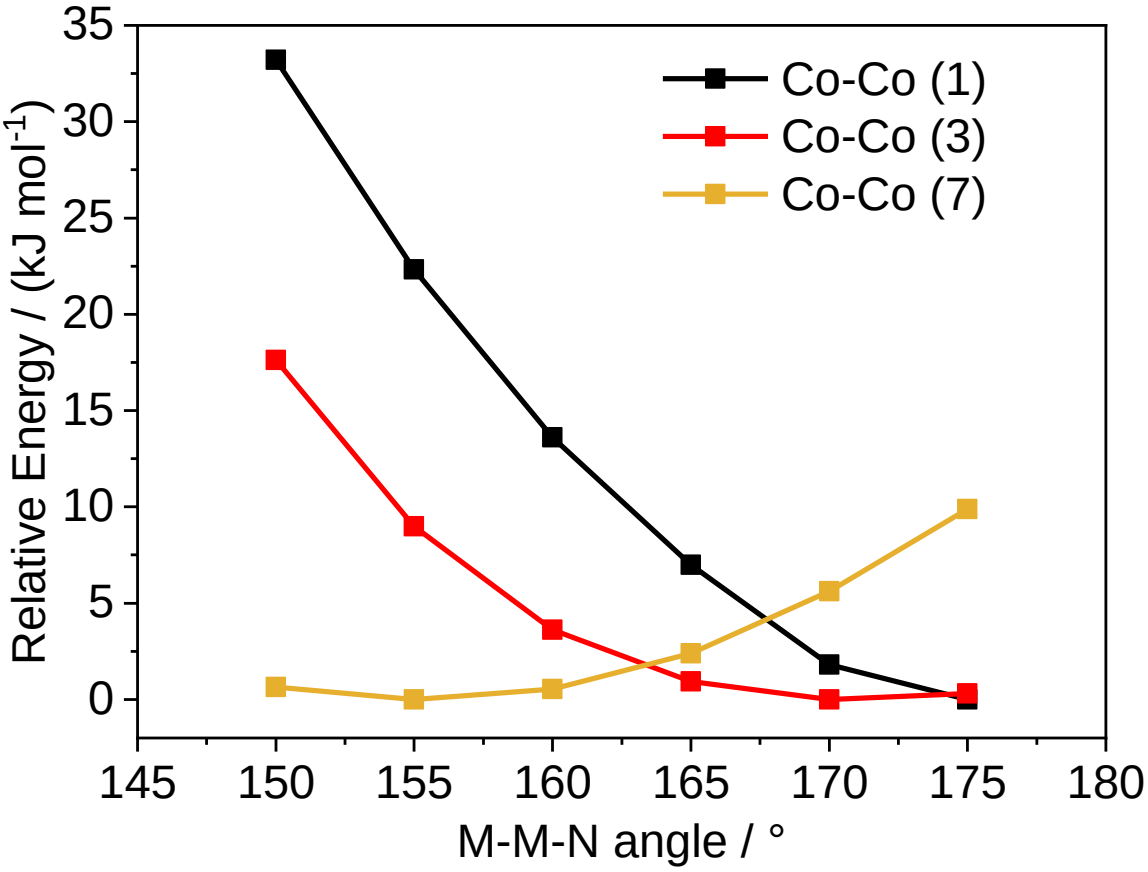

Figure S22. Constrained geometry scans of the M-M-N for the representative Co paddle wheel molecules.

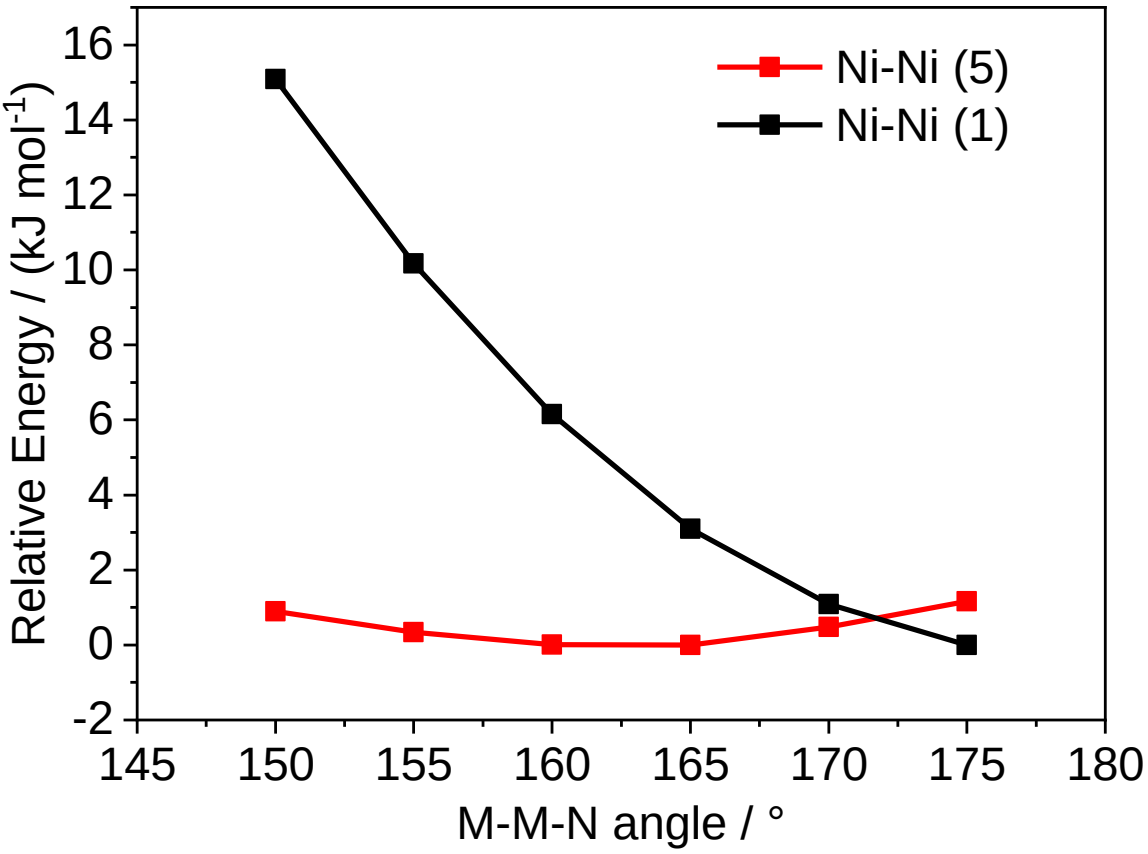

Figure S23. Constrained geometry scans of the M-M-N for the representative Ni paddle wheel molecules.

12. Spin related framework optimization

Periodic structure of DUT-8(Co) in *op* and *cp* phase. Modelling of the periodic structure of DUT-8(Co) in *op* and *cp* phase was done with cp2k software using density functional theory with PBE exchange correlation functional and empirical D3 dispersion correction. The basis set employed in the calculations was DZVP-MOLOPT-SR-GTH. GGA+U approach has been tested for different spin configuration. In order to access the ferromagnetic ordering a broken symmetry approach has been employed. The uncorrected for self-interaction error PBE exchange-correlation functional gives a wrong magnetic moment per Co ion (2.5 and -0.5 total spin per Co ion in the PW, respectively) in the low-spin state of the PW unit where we expect to have nearly one unpaired electron per Co ion. In the high-spin state (3 unpaired electrons per Co) the magnetic moment per Co ion is correct (total spin 2.7 per Co ion in the PW), but the Co-Co distance in the PW is much shorter, (by 0.32 A) in comparison to the experimental one, while the Co-N distances are longer by ca. 0.1 A. In order to describe the magnetic moment per Co ion correctly, we had to apply DFT+U scheme. In cp2k implementation of DFT+U, we used the method based on Mulliken population analysis. Since U-J parameters for Co, when mixed Gaussian and plane wave basis set are used, are not known we hat to performed a series of calculations for the *op* form of DUT-8(Co) in the low-spin state (one unpaired electron per Co) using U-J parameter for Co(d) ranging from 0.5 to 3.5 eV with step of 0.2 eV. The results are shown in Figure S24.

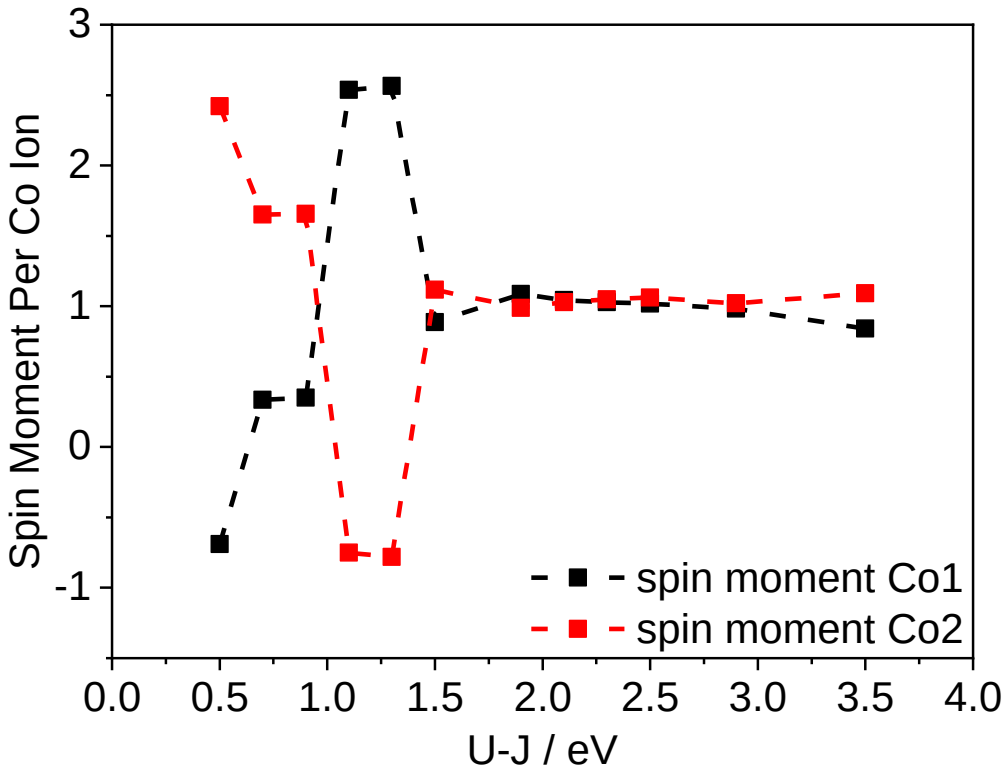

Figure S24. Spin moment per each of the two Co ion in the paddle wheel unit for periodic system of DUT-8(Co), modelled in low-spin state with total number of two unpaired electrons per PW unit as a function of the U-J parameter applied for Co(d) states.

From Figure S24 is visible that for U-J values in the range 2.0 – 2.9 eV the two Co ion show equivalent spin moment, close to one unpaired electron per Co ion in the PW. In this way we concluded that U-J parameter around 2.2 eV is the lowest one, which gives proper electron localization on the d-states of the Co ions.

If we denote with E(total) the total energy of *cp* and *op*, E(disp) only the dispersion energy from DFT-D3 in *op* and *cp*. Than we calculate the difference [E(total) – E(disp)]*op* and [E(total) – E(disp)]*cp*, now the strain is defined as E(str) = [E(total) – E(disp)]*cp* – [E(total) – E(disp)]*op*, which is basically electronic energy + nuclear repulsion energy for each form *op* and *cp*, respectively. In such a way the strain is an estimate for the energy penalty in the *cp* phase due to the deformation of the structure (bonds, angles etc.).

Table S1. Total energies for all calculated spin states in the *op* and *cp* phase of DUT-8(Co). The energy difference ΔE(*cp*-*op*)) kJ mol^{-1} is calculated between the most stable *op* and *cp* phases (marked in bold).

	Total energy / Hartree	ΔE (*cp*-*op*) / kJ mol^{-1}	ΔE(disp) (*cp*-*op*) / kJ mol^{-1}	E(str) (*cp*-*op*) / kJ mol^{-1}	Spin moment Co1	Spin moment Co2	R(Co..Co) / pm	R(Co-N) / pm	Co-Co-N angle / °
Experimental data							**269**	**211/211**	**172/172**
open forms									
open shell singlet	-624.0756057				0.0	0.0			
ns=0 (closed shell)	-624.0756072				0.0	0.0	228	224/224	179/176
ns=2	-624.0645392				-0.6	2.3	243	212/224	178/176
ns=6	-624.0562591				2.6	2.6	237	221/226	172/173
DFT+U (U-J=2.2 ev)									
open shell singlet ns=2	-623.9851420				1.0	-0.9	250	220/241	178/175
open shell singlet ns=6	-624.0117527				2.8	-2.8	285	220/211	177/175
ns=2	-623.9675537				1.0	1.0	239	202/241	178/176
ns=6	**-624.0196218**				**2.8**	**2.7**	**279**	**212/206**	**178/176**
closed forms									
open shell singlet	-624.0829314	-19	-177	158	2.5	-2.5	260	216/214	160/160
ns=0 (closed shell)	-624.0851531	-25	-182	157	0.0	0.0	233	227/228	170/169
ns=2	-624.0830286	-49	-185	137	-0.6	2.3	245	221/217	163/167
ns=6	-624.0828891	-70	-181	111	2.6	2.6	259	218/217	160/159
DFT+U (U-J=2.2 ev)									
open shell singlet ns=6	**-624.0542901**	**-91**	**-175**	**84**	**2.8**	**-2.8**	**288**	**214/212**	**159/158**

13. Additional simulated UV-vis spectra

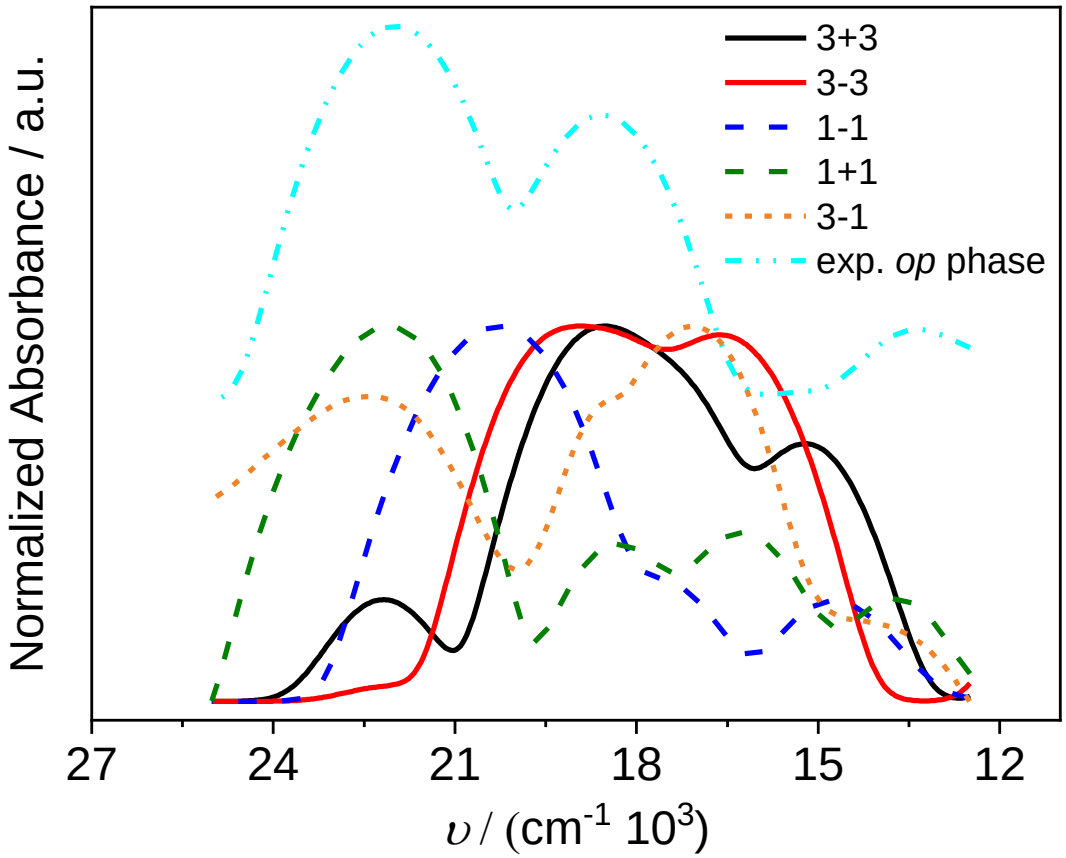

Figure S25. Simulated UV-vis spectra for the *open pore* phase of DUT-8(Co) in comparison to the experimental spectrum (cyan). The numbers correspond to the number of unpaired electrons per Co^{2+} ion. The "+" represents a ferromagnetic coupling and the "-" an antiferromagnetic coupling respectively.

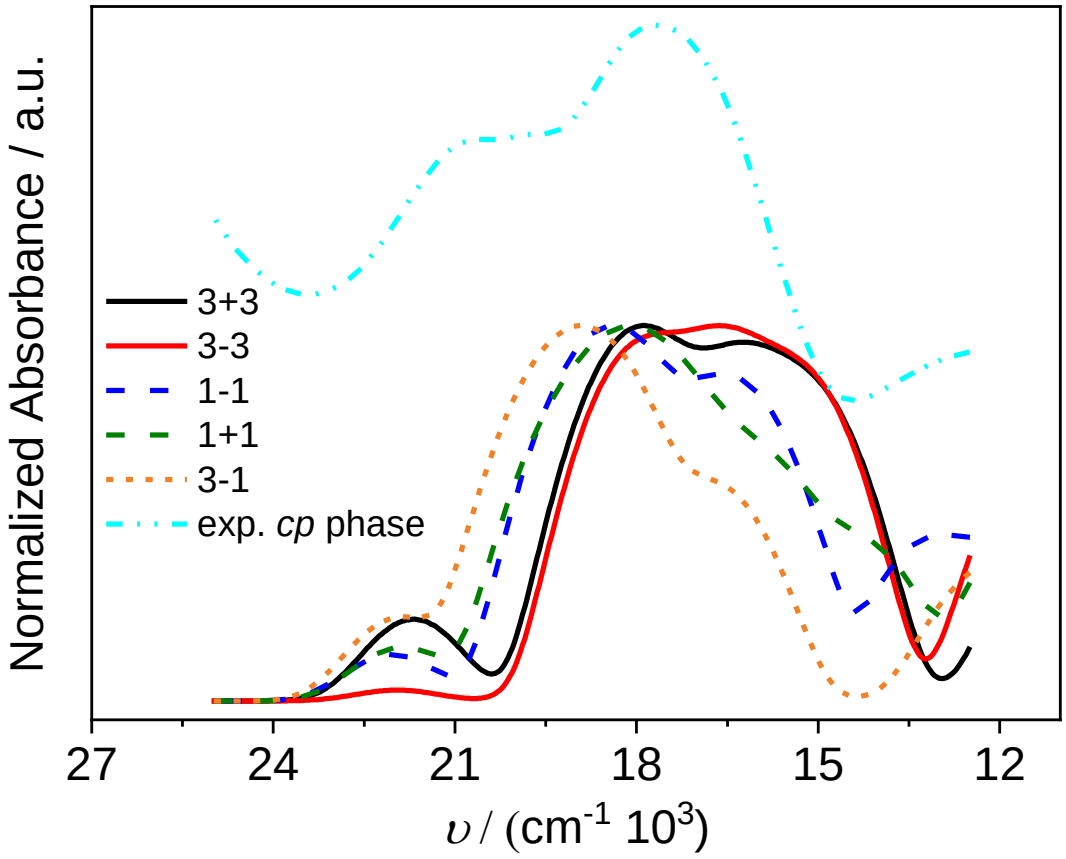

Figure S26. Simulated UV-vis spectra for the *closed pore* phase of DUT-8(Co) in comparison to the experimental spectrum (cyan). The numbers correspond to the number of unpaired electrons per Co^{2+} ion. The "+" represents a ferromagnetic coupling and the "-" an antiferromagnetic coupling respectively.